Raman spectra of putrescine, spermidine and spermine polyamines and their N-deuterated and N-ionized derivatives

ARTICLE *in* JOURNAL OF RAMAN SPECTROSCOPY · APRIL 2003

Impact Factor: 2.67 · DOI: 10.1002/jrs.1001

3 AUTHORS:

António M Amorim Da Costa
University of Coimbra
60 PUBLICATIONS **646** CITATIONS
SEE PROFILE

Maria PM Marques
University of Coimbra
123 PUBLICATIONS **2,404** CITATIONS
SEE PROFILE

Luis A E Batista de Carvalho
University of Coimbra
88 PUBLICATIONS **919** CITATIONS
SEE PROFILE

JOURNAL OF RAMAN SPECTROSCOPY
J. Raman Spectrosc. 2003; **34**: 357–366
Published online in Wiley InterScience (www.interscience.wiley.com). DOI: 10.1002/jrs.1001

JRS

Raman spectra of putrescine, spermidine and spermine polyamines and their *N*-deuterated and *N*-ionized derivatives

A. M. Amorim da Costa,[1]* M. P. M. Marques[1,2] and L. A. E. Batista de Carvalho[1]

[1] Unidade I&D 'Química-Física Molecular,' University of Coimbra, 3000 Coimbra, Portugal
[2] Department of Biochemistry, Faculty of Sciences and Technology, University of Coimbra, 3000 Coimbra, Portugal

Received 14 November 2002; Accepted 1 February 2003

The experimental and calculated Raman spectra of the *N*-hydrogenated and *N*-deuterated biogenic polyamines putrescine, spermidine and spermine and of their *N*-hydrogenated and *N*-deuterated hydrochloride salts in the 2000–3400 cm^{-1} spectral region (at distinct temperatures) are reported and analysed. A complete assignment of the N–H, C–H and N–D stretching modes is carried out, in the light of both steric and hydrogen-bonding interactions on the conformational behaviour of these systems.

KEYWORDS: putrescine; spermidine; spermine; conformational analysis; polyamines

INTRODUCTION

Putrescine [1,4-butanediamine, $H_2N(CH_2)_4NH_2$], spermidine [*N*-(3-aminopropyl)-1,4-butanediamine, $H_2N(CH_2)_4NH(CH_2)_3NH_2$], formed from putrescine, and spermine [*N*,*N*′-bis(3-aminopropyl)-1,4-butanediamine, $H_2N(CH_2)_3NH(CH_2)_4NH(CH_2)_3NH_2$] are biogenic polyamines present in all eukariotic organisms, which play an essential role in cell growth and differentiation and in the immunological system. Because of the basic nature of the amine groups, these compounds are prone to interact (mainly in their protonated cationic forms) with the phosphonate groups of nucleic acids.[1–3] Although the exact nature of the biochemical mechanism through which these aliphatic linear amines act in the living cell is still unknown, the relative importance of intra- and intermolecular interactions has proved to be one of the utmost importance in determining the conformational preferences of this kind of systems, either as pure compounds or in solution.[4–6]

From a biosynthesis point of view, putrescine is the precursor of the larger analogues spermidine and spermine, the comparative study of these three polyamines under similar conditions therefore being useful. A series of conformational analyses using Raman vibrational spectroscopy and MO *ab initio* calculations, already carried out by the authors for 1,2-diaminoethane ($H_2N(CH_2)_2NH_2$),[4] and also for 1,4-butane diamine ($H_2N(CH_2)_4NH_2$)[5,6] and 1,6-hexanediamine ($H_2N(CH_2)_6NH_2$),[7] have yielded relevant information which will be used in the present study in order to achieve a better understanding of the structural behaviour of the tri- and tetraamines spermidine and spermine.

Apart from a Raman and infrared (IR) study reported on spermidine and spermine interactions with hydrochloric and phosphoric acids,[1] a theoretical conformational analysis of putrescine[5] and a thorough vibrational study [by both Raman and inelastic neutron scattering (INS) spectroscopy] of the $H_2N(CH_2)_nNH_2$ (n = 1–10 and 12), polyamines spermidine and spermine (in their unprotonated, protonated and *N*-deuterated forms) in the low-wavenumber region,[6] only a preliminary assignment of the Raman spectrum of putrescine, in aqueous solution, is to be found in the literature.[8] Actually, the assignment of the vibrational bands of polyamines and their hydrochloride salts, due to the stretching modes involving the hydrogen atoms, is uncertain and has been little discussed in the literature because of their complexity.

The present work is a tentative approach in such a direction, dealing with the analysis of the Raman spectra of putrescine, spermidine and spermine in the 2000–3400 cm^{-1} region, in the light of steric and hydrogen-bonding effects on the corresponding molecular rearrangements. This paper is focused mainly on the interpretation and discussion of the N–H, C–H and N–D stretching vibrational modes,

*Correspondence to: A. M. Amorim da Costa, Unidade I&D 'Química-Física Molecular,' University of Coimbra, 3000 Coimbra, Portugal. E-mail: acosta@ci.uc.pt
Contract/grant sponsor: Portuguese Foundation for Science and Technology; Contract/grant number: POCTI/33199/QUI/2000.
Contract/grant sponsor: European Community Fund FEDER.

for *N*-hydrogenated and *N*-deuterated polyamines, both in the neutral and in the hydrochloride (polycationic) forms.

EXPERIMENTAL

Raman spectroscopy

The Raman spectra were measured at room temperature on a Spex Ramalog 1403 double spectrometer (focal distance 0.85 m, aperture $f/7.8$) equipped with holographic gratings of 1800 grooves mm^{-1} and a detector assembly containing a thermoelectrically cooled Hamamatsu R928 photomultiplier tube. The spectrometer operated with slits of 320 μm and at 1 cm^{-1} s^{-1}. Below room temperature (ca 220 K), a laboratory-made Harney–Miller type assembly was used, in a triple monochromator Jobin-Yvon T64000 Raman system (0.640 m, $f/7.5$) with holographic gratings of 1800 grooves mm^{-1}. The detection system was a non-intensified charge coupled device (CCD) and the entrance slit was set to 300 μm.

Radiation of 514.5 nm from an argon ion laser (Coherent, Innova 300) was used for excitation, providing 100–120 mW at the sample position. Samples were sealed in Kimax glass capillary tubes of 0.8 mm i.d.. Under the above conditions, the error in wavenumbers was estimated to be within 1 cm^{-1} and the error in temperatures was less than 1 K.

Ab initio MO calculations

The *ab initio* calculations were carried out with the Gaussian 98W program,[9] within the density functional theory (DFT) approach, using the B3LYP method,[10–15] which includes a mixture of Hartree–Foch (HF) and DFT exchange terms. The gradient-corrected correlation functional was used[16,17] (parameterized after Becke[18,19]), along with the double-zeta split valence basis set 6–31G*.[20]

Only the geometries with all skeletal dihedral angles equal to 180° (all-*trans*) were considered in the present work. Molecular geometries were fully optimized by the Berny algorithm, using redundant internal coordinates.[21] The bond lengths to within ca 0.1 pm and the bond angles to within ca 0.1°. The final root-mean-square (r.m.s.) gradients were always less than 3×10^{-4} hartree $bohr^{-1}$ or hartree rad^{-1}.

Chemicals

Putrescine, spermidine and spermine and their hydrochloride salts were purchased from Sigma-Aldrich (Sintra, Portugal). The deuterated compounds were obtained by solubilization of the amines in D_2O (ca 10% excess) followed by distillation under vacuum (this process being repeated at least three times). Purification of the samples was carried out shortly before running the Raman spectra. The solid uncharged amines were purified by sublimation, while the liquids were distilled under vacuum. The salts were recrystallized (sometimes repeatedly) from ethanol–water (1 : 1) (being obtained as white needles). Air- or moisture-sensitive samples (both the uncharged and the deuterated amines) were always handled in a glove-box, under a nitrogen or argon atmosphere.

RESULTS AND DISCUSSION

N–H stretching wavenumbers

Tables 1–3 give the experimental and calculated vibrational wavenumbers for solid *N*-hydrogenated and *N*-deuterated putrescine, spermidine, spermine and their hydrochlorides, in the high-wavenumber region. On the basis of the theoretical results and previously reported assignments for solid putrescine and similar linear diamines,[1,5,7,23] the observed Raman bands at 3200–3350 cm^{-1} were ascribed to the symmetric and antisymmetric stretching of the N—H oscillators, i.e. NH and NH_2 groups. The Raman band detected between 3150 and 3175 cm^{-1} for all neutral non-deuterated species can reasonably be attributed to the N–H stretching modes of both the primary and secondary hydrogen-bonded $NH_2\cdots N$ and $NH\cdots N$ amine groups. These assignments are well supported by the observed N–D stretching wavenumbers in the 2300–2500 cm^{-1} wavenumber range, which display the expected decrease of ca 1.37 times in the corresponding wavenumber values (Figs 1–3).

As observed previously for other amine hydrochlorides,[1] most of the bands in the 3150–3350 cm^{-1} wavenumber region are absent in the Raman spectra of putrescine, spermidine and spermine hydrochloride species: these samples exhibit only a weak and broad signal below 3150 cm^{-1} (Figs 1–3). In fact, the ionization of the primary and secondary amine groups (yielding NH_3^+ and NH_2^+), which involves the formation of $N^+—H\cdots Cl^-$ type hydrogen bonds and a significant increase in bond polarization, and also a decrease in bond strength, is probably responsible for the detected drastic changes in the intensity of those features, and for their shift to lower wavenumbers. Actually, from the observed values of the N–D stretching wavenumbers of the ionized amine groups in the corresponding *N*-deuterated hydrochlorides, the expected wavenumbers for the N–H stretching would be around 2980–3150 cm^{-1}. Despite several weak features thus detected in this region, the strong band observed at ca 2982 cm^{-1} in the spectra of all hydrochlorides (both *N*-deuterated and non-deuterated) (Figs 1–3), previously ascribed by Mureinik and Scheuermann[24] to the N–H stretching mode (through analysis of the Raman spectrum of ethylenediamine dihydrochloride), cannot, in the light of the results obtained here, be assigned to this vibrational mode, as it does not disappear upon deuteration of the NH_3^+ groups. In turn, as discussed below, this band should be mainly associated with C–H stretching modes of the $CH_2—N^+$ groups, as proposed by Kalyanasundaram and Thomas[25] from a Raman study of alkylammonium chlorides.

Table 1. Experimental Raman (solid phase) and calculated wavenumbers and intensities (in the 2000–3500 cm^{-1} region) for putrescine and putrescine dihydrochloride

	Calculated[a]		
Experimental/cm^{-1}	Raman[b]/cm^{-1}	Infrared[c]/cm^{-1}	Assignment
N-Hydrogenated putrescine (C_{2h}):			
2639 (w)[d]			
2705 (m)			
2846 (s)	2890 (148, A_g)		CH_2 sym. stretching (FR)
		2894 (37, B_u)	
2860 (s)	2918 (165, A_g)		CH_2 sym. stretching (FR)
		2921 (120, B_u)	
2890 (vs)	2912 (152, B_g)		CH_2 asym. stretching
		2928 (13, A_u)	
2916 (m)			2 × CH_2 scissoring (FR)
2933 (m)			2 × CH_2 scissoring (FR)
		2964(136, A_u)	
3171 (m)			NH···N sym. stretching
3255 (w)	3316 (186, A_g)		NH_2 sym. stretching
		3317 (5, B_u)	
3329 (s)	3397 (112, B_g)		NH_2 asym. stretching
		3398 (2, A_u)	
N-Deuterated putrescine (C_{2h}):			
2337 (s)	2398 (102, A_g)		ND_2 sym. stretching
2386 (vw)			
2430 (w)			
2475 (m)	2502 (63, B_g)		ND_2 asym. stretching
2511 (w)			
2655 (vw)			
2720 (w)			
2735 (w)			
2846 (s)	2890 (148, A_g)		CH_2 sym. stretching (FR)
		2894 (37, B_u)	
2857 (s)	2920 (156, A_g)		CH_2 sym. stretching (FR)
		2922 (121, B_u)	
2885 (vs)	2912 (150, B_g)		CH_2 asym. stretching
		2928 (14, A_u)	
2910 (m)			2 × CH_2 scissoring (FR)
2933 (m)			2 × CH_2 scissoring (FR)
		2964 (137, A_u)	
N-Hydrogenated putrescine dihydrochloride (C_{2h}):			
2789 (m)			
2883 (s)	2926 (147, A_g)		CH_2 sym. stretching (FR)
		2936 (12, B_u)	
2906 (m)			2 × CH_2 scissoring (FR)
2930 (vs)	2965 (108, B_g)		CH_2 asym. stretching
2977 (sh)			
		2983 (9, A_u)	
2980 (vs)	2990 (122, A_g)		NCH_2 sym. stretching

(*continued overleaf*)

Table 1. (*Continued*)

Experimental/cm^{-1}	Calculated[a] Raman[b]/cm^{-1}	Calculated[a] Infrared[c]/cm^{-1}	Assignment
		2991 (1, B_u)	
	3047 (68, B_g)		
3036 (w,b)			N–H···Cl stretching
3073 (w,b)			N–H···Cl stretching
	3245 (161, A_g)	3244 (152, B_u)	NH_3^+ sym. stretching
	3322 (98, A_g)	3322 (253, B_u)	NH_3^+ asym. stretching
	3329 (61, B_g)	3329 (217, A_u)	NH_3^+ asym. stretching
N-Deuterated putrescine dihydrochloride (C_{2h}):			
2175 (m)			N–D···Cl sym. stretching
2211 (w)			N–D···Cl sym. stretching
2239 (w)			
2270 (w)			
2287 (m)			N–D···Cl asym. stretching
2301 (m)			N–D···Cl asym. stretching
2328 (sh)			
	2326 (80, A_g)	2325 (91, A_u)	ND_3^+ sym. stretching
	2451 (50, A_g)	2451 (137, B_u)	ND_3^+ asym. stretching
	2456 (34, B_g)	2456 (112, A_u)	ND_3^+ asym. stretching
2636 (vw)			
2786 (w)			
2883 (s)	2927 (146, A_g)		CH_2 sym. stretching (FR)
		2936 (12, B_u)	
2910 (m)			2 × C-H_2 scissoring (FR)
2929 (vs)	2965 (107, B_g)		CH_2 asym. stretching
2977 (sh)			
		2983 (11, A_u)	
2980 (vs)	2991 (117, A_g)		NCH_2 sym. stretching
		2991 (1, B_u)	
	3047 (65, B_g)		

[a] For an all-*trans* conformation, at the B3LYP/6–31G* level of calculation; wavenumbers scaled by a factor of 0.9614.[22]

[b] Raman scattering activities in Å u^{-1}.

[c] Infrared intensities in km mol^{-1}.

[d] Abbreviations: s = strong; m = medium; w = weak; v = very; sh = shoulder; b = broad; FR = Fermi resonance.

C–H stretching wavenumbers

The analysis of the C–H stretching region (2800–3000 cm^{-1}) of the experimental Raman spectra for putrescine, spermidine, spermine and their hydrochloride salts shows that the deuteration of the amino groups has no significant effects on either the wavenumbers or the number of bands associated with the methylene stretching modes. In fact, upon *N*-deuteration only some small changes in the relative band intensity are detected. In turn, both the wavenumber values and the relative intensity of the observed features (in this same spectral region) as the number of CH_2 groups in the hydrocarbon chain increases are noticeable and complex (Figs 1–3).

Several FTIR and Raman studies have already been reported for the simplest linear diamines and their *N*-deuterated and hydrochloride derivatives.[26–29] The generally accepted assignment is as follows: the fundamental methylene C–H symmetric stretch occurs at ca 2860 cm^{-1} (Figs 1–3), features due to Fermi resonance interaction between this mode and overtones of the CH_2 scissoring A_g vibrations being observed at about 2915 and 2930 cm^{-1}. The band at ca 2890 cm^{-1} is ascribed to the B_{1g} antisymmetric methylene C–H stretching, which is floating on top of a broad background of the A_g species.[26,30]

It is well known[31–33] that whenever *gauche* structures are present, the *trans* overtone levels around 2900 cm^{-1} are

Table 2. Experimental Raman (solid phase) and calculated wavenumbers and intensities (in the 2000–3500 cm^{-1} region) for spermidine and spermidine trihydrochloride

Experimental/ cm^{-1}	Calculated[a]/ cm^{-1}	Assignment
N-Hydrogenated spermidine (C_1):		
2689 (w)[b]		
2715 (w)		
2761 (m)		
2798 (m)		
2850 (s)	2893 (161; 9)	CH_2 sym. stretching (FR)
2890 (vs)	2928 (97; 116)	CH_2 asym. stretching
2925 (sh)		2 × CH_2 scissoring (FR)
2939 (sh)		2 × CH_2 scissoring (FR)
2960 (sh)		2 × CH_2 scissoring (FR)
3160 (m)		N–H···N stretching
3250 (w)	3319 (147; 4)	NH_2 sym. stretching
3294 (s)	3327 (53; 2)	N–H stretching
3326 (vs)	3398 (103; 2)	NH_2 asym. stretching
N-Deuterated spermidine (C_1):		
2330 (s)	2398 (71; 0)	ND_2 sym. stretching
2440 (m)	2431 (31; 0)	N–D stretching
2473 (s)	2503 (60; 0)	ND_2 asym. stretching
2718 (w)		
2762 (m)		
2797 (m)		
2848 (s)	2892 (67; 21)	CH_2 sym. stretching (FR)
2861 (sh)	2893 (160; 9)	CH_2 sym. stretching (FR)
2890 (vs)	2929 (92; 116)	CH_2 asym. stretching
2924 (sh)		2 × CH_2 scissoring (FR)
2938 (sh)		2 × CH_2 scissoring (FR)
N-Hydrogenated spermidine trihydrochloride (C_s):		
2682 (sh)		
2755 (w)		
2798 (w)		
2808 (sh)		
2821 (sh)		
2873 (m)	2927 (125; 0; *A′*)	CH_2 sym. stretching (FR)
2914 (vs)	2966 (96; 0; *A″*)	CH_2 asym. stretching
2933 (s)	2931 (91; 3; *A′*)	CH_2 sym. stretching
2952 (w)		2 × CH_2 scissoring (FR)
2980 (s)	2986 (52; 1; *A′*)	NCH_2 sym. stretching
2986 (s)	2991 (97; 0; *A′*)	NCH_2 sym. stretching
3021 (sh,b)		N–H···Cl stretching
3205 (vw,b)	3233 (78; 109; *A′*)	NH_3^+ sym. stretching
	3255 (45; 38; *A′*)	NH_2^+ sym. stretching
	3308 (21; 57; *A″*)	NH_2^+ asym. stretching
	3314 (50; 133; *A′*)	NH_3^+ asym. stretching
N-Deuterated spermidine trihydrochloride (C_s):		
2090 (w,b)		N–D···Cl stretching
2185 (m,b)		N–D···Cl stretching
	2323 (44; 51; *A′*)	ND_3^+ sym. stretching
	2359 (23; 22; *A′*)	ND_2^+ sym. stretching
	2443 (13; 27; *A″*)	ND_2^+ asym. stretching
	2444 (26; 73; *A′*)	ND_3^+ asym. stretching
2754 (w,b)		
2776 (w,b)		
2820 (w,b)		
2873 (s)	2927 (124; 0; *A′*)	CH_2 sym. stretching (FR)
2916 (vs)	2966 (95; 0; *A″*)	CCH_2 asym. stretching
2934 (vs)	2931 (91; 3; *A′*)	CCH_2 sym. stretching
2950 (w)		2 × CH_2 scissoring (FR)
2980 (vs)	2987 (48; 0; *A′*)	NCH_2 sym. stretching
2986 (vs)	2991 (94; 0; *A′*)	NCH_2 sym. stretching

[a] For an all-*trans* conformation, at the B3LYP/6–31G* level of calculation; wavenumbers scaled by a factor of 0.9614;[22] in parentheses: Raman scattering activities in Å u^{-1}; infrared intensities in km mol^{-1}; symmetry mode.

[b] Abbreviations: s = strong; m = medium; w = weak; v = very; sh = shoulder; b = broad; FR = Fermi resonance.

removed, giving back intensity to the overtone band around 2930 cm^{-1}. The observed wavenumber shifts to lower values and the relative intensity changes as the alkyl hydrocarbon chain length gets longer, in the series of polyamines studied (Figs 1–3), are thus the result of the increase in the percentage of *gauche* conformations due to greater flexibility of the chain (from putrescine to spermidine and spermine). The pattern of the C–H stretching region of *N*-hydrogenated spermidine, spermine and their hydrochloride species (displaying three or more CH_2 groups) may therefore be associated with the *gauche* structures resulting from the conformational rearrangements of the non-equivalent methylene groups within these systems.

In putrescine, the two distinct peaks at 2846 and 2860 cm^{-1} are assigned to the fundamental symmetric C–H stretching modes of the CH_2 bonded to the head amino groups of the molecule and to those located in the middle of the chain, respectively. The band at 2890 cm^{-1}, in turn, corresponds to the antisymmetric C–H stretching vibration of those same groups (Fig. 1). Going from the methylenes adjoining the amino groups to the two central CH_2 groups in the chain, a decrease in the strength of the corresponding stretching vibrations is observed, as expected.

It has long been known that the protonation of an amino group strongly influences the neighbouring methylene moieties within a molecule, namely their Raman C–H stretching wavenumbers. In some amino acids, for instance, such as glycine or β-alanine,[8] these wavenumbers showed an increase of up to 40–60 cm^{-1} on protonation of an adjoining NH_2. Although to a smaller extent, this ionization also affects the other methylene groups in the chain. The

Table 3. Experimental Raman (solid phase) and calculated wavenumbers and intensities (in the 2000–3500 cm^{-1} region) for spermine and spermine tetrahydrochloride

Experimental/ cm^{-1}	Calculated[a]/ cm^{-1}	Assignment
N-Hydrogenated spermine (C_1):		
2685 (vw)[b]		
2709 (vw)		
2730 (sh)		
2764 (m)		
2805 (s)	2805 (173; 122)	CH_2 asym. stretching
2856 (vs)	2891 (150; 8)	CH_2 sym. stretching (FR)
2864 (sh)	2899 (154; 10)	CH_2 sym. stretching (FR)
2892 (vs)	2931 (96; 92)	CH_2 asym. stretching
2904 (vs)	2941 (110; 4)	CH_2 asym. stretching
2930 (sh)		2 × CH_2 scissoring (FR)
3160 (m)		N–H···N stretching
3264 (vw)	3317 (188; 0)	NH_2 sym. stretching
3293 (s)	3327 (68; 1)	N–H out-of-phase stretching
3308 (w)	3327 (39; 3)	N–H in-phase stretching
3332 (s)	3398 (86; 1)	NH_2 asym. stretching
N-Deuterated spermine (C_1):		
2335 (m)	2398 (102; 8)	ND_2 sym. stretching
2440 (m)	2431 (38; 1)	N–D stretching
2460 (sh)		
2481 (m)	2503 (49; 0)	ND_2 asym. stretching
2652 (w,b)		
2709 (w)		
2769 (m)		
2805(m)	2805 (175; 122)	CH_2 asym. stretching
2855 (s)	2891 (149; 8)	CH_2 sym. stretching (FR)
2867 (w)	2899 (155; 10)	CH_2 sym. stretching (FR)
2892 (vs)	2931 (97; 97)	CH_2 asym. stretching
2904 (s)	2941 (102; 3)	CH_2 asym. stretching
2922 (sh)		2 × CH_2 scissoring (FR)
2932 (w)		2 × CH_2 scissoring (FR)
N-Hydrogenated spermine tetrahydrochloride (C_1):		
2709 (w)		
2753 (w)		
2779 (w)		
2803 (w)		
2843(w)		
2881 (s)	2929 (116; 0; *A′*)	CH_2 sym. stretching (FR)
2923 (s)	2932 (158; 1; *A′*)	CCH_2 sym. stretching
2944 (s)	2967 (88; 0; *A″*)	CCH_2 asym. stretching
2974 (sh)		2 × CH_2 scissoring (FR)
2983 (m)	2986 (77; 0; *A′*)	NCH_2 sym. stretching
2990 (m)	2990 (202; 0; *A′*)	NCH_2 sym. stretching
3131 (m)	3230 (166; 229, *A′*)	NH_3^+ sym. stretching
	3254 (86; 77; *A′*)	NH_2^+ sym. stretching
	3308 (40; 114; *A″*)	NH_2^+ asym. stretching
	3316 (64; 256; *A″*)	NH_3^+ asym. stretching
N-Deuterated spermine tetrahydrochloride (C_s):		
2132 (s)		N–D···Cl stretching
2178 (s)		N–D···Cl stretching
2322 (w)	2316 (82; 127; *A′*)	ND_3^+ sym. stretching
2357 (m)	2359 (46; 45; *A′*)	ND_2^+ sym. stretching
	2443 (24; 53; *A″*)	ND_2^+ asym. stretching
	2447 (36; 134; *A″*)	ND_3^+ asym. stretching
2754 (w)		
2783 (w)		
2804 (w)		
2883 (s)	2929 (113; 0; *A′*)	CCH_2 sym. stretching
2923 (s)	2931 (163; 1; *A′*)	CCH_2 sym. stretching
2944 (vs)	2966 (86; 1)	CCH_2 asym. stretching
2972 (w)		2 × CH_2 scissoring (FR)
2982 (m)	2987 (70; 1; *A′*)	NCH_2 sym. stretching
2990 (s)	2991 (198; 0; *A′*)	NCH_2 sym. stretching

[a] For an all-*trans* conformation, at the B3LYP/6–31G* level of calculation; wavenumbers scaled by a factor of 0.9614;[22] in parentheses: Raman scattering activities in Å u^{-1}; infrared intensities in km mol^{-1}; symmetry mode.

[b] Abbreviations: s = strong; m = medium; w = weak; v = very; sh = shoulder; b = broad; FR = Fermi resonance.

electrostatic interactions resulting from nitrogen protonation in the molecules investigated here, and also the formation of strong N^+—H···Cl^- intermolecular hydrogen bonds, are known to lead to a tighter molecular packing of the linear polyamine chains in the cationic species as compared with their non-ionized analogues. In this closer packing, the interactions between the carbon and hydrogen atoms are more effective, giving rise to a general upward displacement of the methylene C–H stretching wavenumbers in the Raman spectra. This shift, clearly detected in the present spectra (Figs 1–3), fully supports the assignment of the 2980 cm^{-1} signal to the C–H stretching mode of these CH_2—H_3N^+ groups. In fact, a general blue shift (of about 40 cm^{-1}) is observed for the *N*-hydrogenated and *N*-deuterated putrescine, spermidine and spermine hydrochlorides, with particular evidence for the appearance of a perfectly isolated band at ca 2980 cm^{-1}, which is not seen for the neutral systems.

In turn, *N*-deuteration of the primary and secondary amine groups of the polyamines studied, in both the neutral and positively charged forms, was not shown to affect the general band pattern (either in intensity or wavenumber) in the 2800–3000 cm^{-1} region of the spectra [Figs 1–3, (a) and (c) vs (b) and (d)].

Linear n-alkane crystals are known to exist mostly in the all-*trans* conformation,[34] sometimes hosting small distortions due to different possible *gauche* arrangements. In the solid,

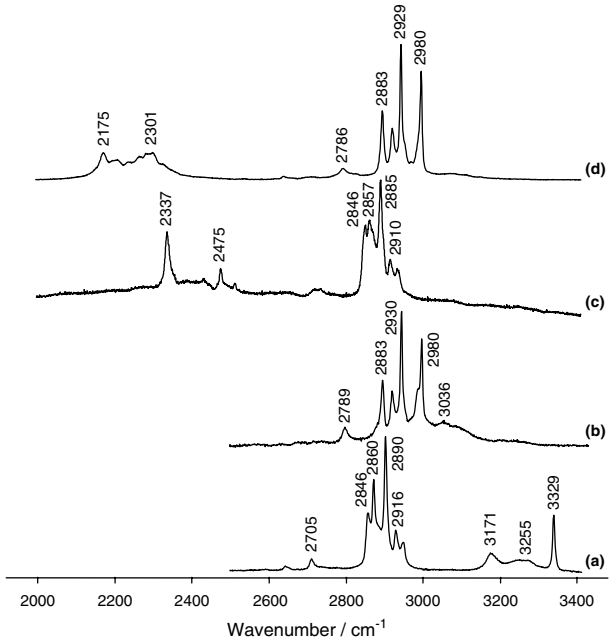

Figure 1. Raman spectra (2000–3400 cm^{-1}), N–D, C–H and N–H stretching modes, for solid: (a) *N*-hydrogenated putrescine; (b) *N*-hydrogenated putrescine dihydrochloride; (c) *N*-deuterated putrescine; and (d) *N*-deuterated putrescine dihydrochloride.

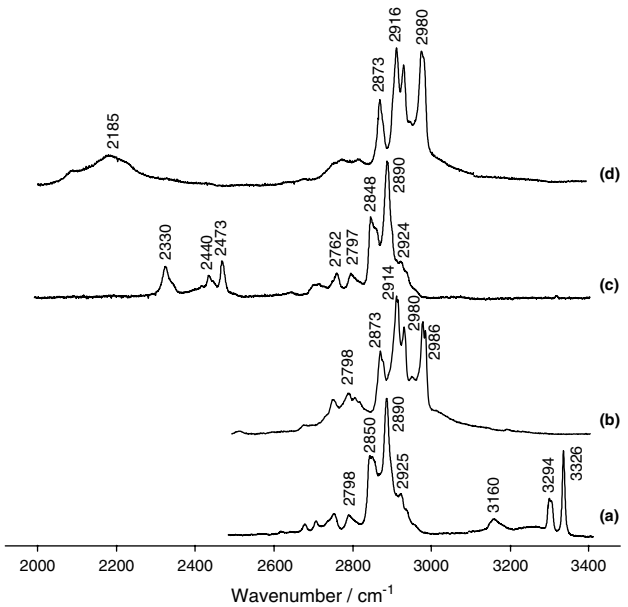

Figure 2. Raman spectra (2000–3400 cm^{-1}), N–D, C–H and N–H stretching modes, for solid: (a) *N*-hydrogenated spermidine; (b) *N*-hydrogenated spermidine trihydrochloride; (c) *N*-deuterated spermidine; and (d) *N*-deuterated spermidine trihydrochloride.

the amount of these conformational distortions increases as the hydrocarbon chain lengthens. Such an effect becomes

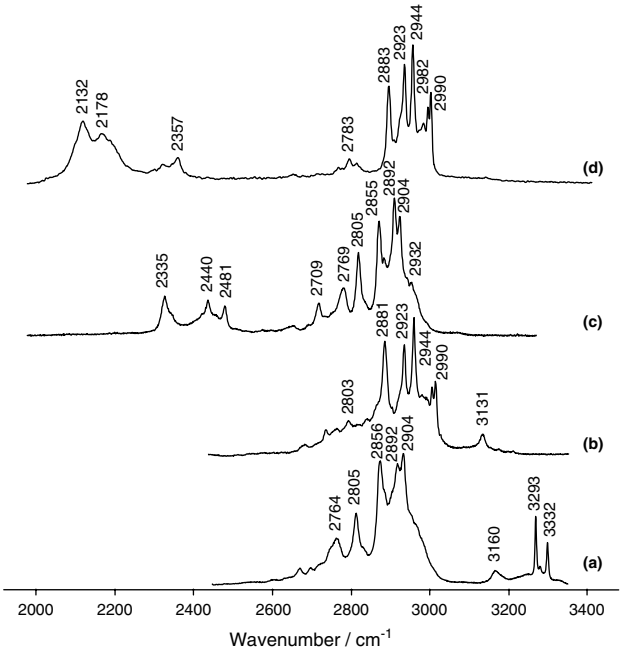

Figure 3. Raman spectra (2000–3400 cm^{-1}), N–D, C–H and N–H stretching modes, for solid: (a) *N*-hydrogenated spermine; (b) *N*-hydrogenated spermine tetrahydrochloride; (c) *N*-deuterated spermine; and (d) *N*-deuterated spermine tetrahydrochloride.

dominant in the liquid state, approaching 100% in the gas phase. As has been widely proved, these distortions in the hydrocarbon chains, with either increasing chain length or increasing temperature, which involve phase transitions, can be probed by the relative intensity changes observed in the Raman C–H stretching bands.[35] In fact, the present experimental observations in the polyamines under investigation (that may be well compared to an n-alkane, mainly in their totally protonated form) show that, upon melting, the Raman signal corresponding to the C–H symmetric stretching mode (ca 2855 cm^{-1}) becomes the strongest feature in the liquid, while the band ascribed to the antisymmetric mode (ca 2904 cm^{-1}) shifts upwards (Fig. 4), in accordance with previously reported studies on several *trans* hydrocarbon chains.[32]

The sensitivity of amine C–H stretching band intensity to the conformational characteristics of these compounds is a complex matter, and has been widely analysed.[36–38] From experimental frequency–phase difference curves, plotted for the CH_2 symmetric and antisymmetric stretching vibrations of n-alkanes,[30,35,39,40] it was concluded that the Raman band corresponding to the antisymmetric mode is superimposed to a broad, non-negligible, background signal due to CH_2 scissoring overtones intensified through Fermi resonance interaction with the methylene in-phase C–H stretching fundamental, as discussed previously. Hence even small

JRS

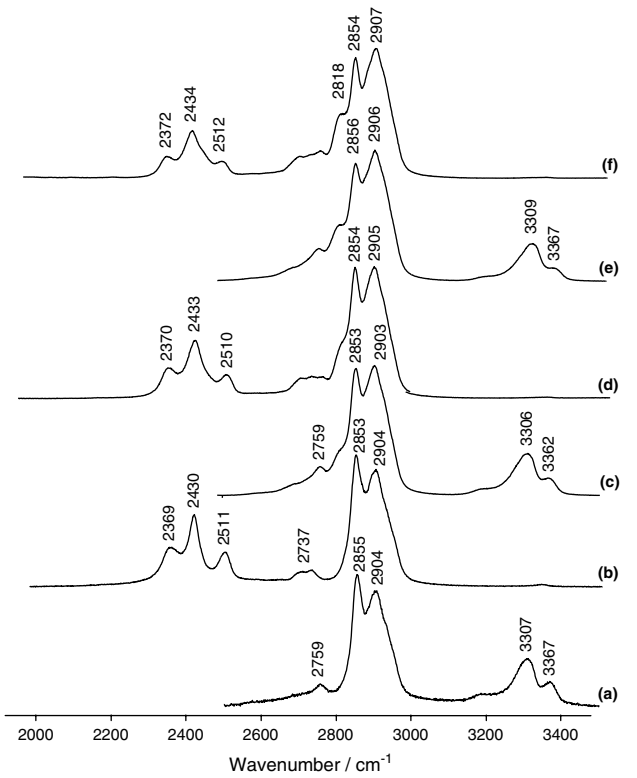

Figure 4. Raman spectra (2000–3500 cm^{-1}), N–D, C–H and N–H stretching modes, for liquid: (a) *N*-hydrogenated putrescine (303 K); (b) *N*-deuterated putrescine (295 K); (c) *N*-hydrogenated spermidine (295 K); (d) *N*-deuterated spermidine (295 K); (e) *N*-hydrogenated spermine (303 K); and (f) *N*-deuterated spermine (295 K).

wavenumber changes in the methylene scissoring fundamental upon formation of *gauche* isomers lead to the removal of this resonance condition, which results in a decrease in the observed maximum of the feature comprising both the overtones (broad signal) and the superimposed, intense, narrow C–H antisymmetric stretching band, but hardly affecting the intensity of the corresponding symmetric mode. On this basis, it is possible to use the variation of the intensity (assumed as the measured band height) ratio between the C–H symmetric and antisymmetric stretching modes as a measure of the conformational changes within the polyamine. Breaking the total relative intensity measured by such a ratio into three parts, (i) the residual intensity in the liquid (= 0.7), (ii) the difference between the intensity of a liquid and that of an isolated all-*trans* chain and (iii) the intensity due to vibrational coupling between the adjacent chains, the lateral interactions, Gaber and Peticolas[41] proposed a quantitative parameter for measuring the effect due to vibrational coupling between adjacent chains, by using a simple C–H antisymmetric vs symmetric stretching peak height ratio (r). This distortion parameter, represented by

$$S = (r - 0.7)/1.5 \quad (1)$$

is only approximate and must be considered semi-quantitative, but it will give some insight into the amount of lateral interaction for analogous compounds with different chain lengths, even within the same physical state.

Table 4 gives this kind of S values determined for both the solid and liquid *N*-hydrogenated and *N*-deuterated polyamines, studied and also for their hydrochloride derivatives. These results correspond to temperatures ranging from room temperature (295 K) to 248 K for *N*-deuterated putrescine and spermine, a few degrees below the melting-points of these compounds. For the hydrochloride salts (both *N*-deuterated and non-deuterated), values were obtained for 295 K, more than 250 K below the melting-points. The results presented for the liquid state, in turn, were determined for a very short temperature range, 295–303 K, roughly 3–10 K above the melting-points.

From these values, it appears that, for the same molecule, in either the solid or liquid state, the effect of nitrogen deuteration on the degree of distortion of the hydrocarbon chain is small. Nevertheless, it is also evident that the non-deuterated amines putrescine and spermidine are slightly less prone to displacement from the all-*trans* geometry than their *N*-deuterated counterparts, in both the neutral and the protonated species. In fact, the more compact arrangement of the *N*-hydrogenated species, due to intermolecular NH···N hydrogen bonds, is responsible for this greater resistance to distortion, as it explains the higher melting temperatures of these compounds relative to their *N*-deuterated analogues

Table 4. The S order/disorder parameter determined for both solid and liquid *N*-hydrogenated and *N*-deuterated putrescine, spermidine and spermine, and their hydrochloride derivatives

Compound	T/K	S
Solid state		
N-Hydrogenated putrescine	295	0.72
N-Deuterated putrescine	248	0.72
N-Hydrogenated spermidine	258	0.68
N-Deuterated spermidine	263	0.66
N-Hydrogenated spermine	295	0.24
N-Deuterated spermine	248	0.34
N-Hydrogenated putrescine dihydrochloride	295	0.89
N-Deuterated putrescine dihydrochloride	295	0.84
N-Hydrogenated spermidine trihydrochloride	295	0.64
N-Deuterated spermidine trihydrochloride	295	0.62
N-Hydrogenated spermine tetrahydrochloride	295	0.34
N-Deuterated spermine tetrahydrochloride	295	0.46
Liquid state		
N-Hydrogenated putrescine	303	0.29
N-Deuterated putrescine	295	0.29
N-Hydrogenated spermidine	295	0.22
N-Deuterated spermidine	295	0.20
N-Hydrogenated spermine	303	0.28
N-Deuterated spermine	295	0.25

(the ND···N interactions being known to be significantly weaker than the NH···N interactions). For the larger tetraamine spermine, however, this trend is not maintained, most probably owing to the presence of four nitrogen atoms, and to its greater flexibility compared with the smaller putrescine and spermidine, which renders NH···N interactions between chains less prone to occur, the all-*trans* extended orientation of the molecule thus being less favoured.

The values now obtained for the percentage of *trans* content for solid putrescine, spermidine and spermine clearly show that the molecular conformation of these polyamines is not always a rigorously all-*trans* arrangement. When going from the solid to the liquid state, the degree of lateral distortion in the hydrocarbon chain increases by more than 50% for both putrescine and spermidine, but only ca 10% for spermine (Table 4).

For the hydrochloride salts, in turn, a very high degree of all-*trans* conformation is expected, owing to the presence of strong interchain N^+—H···Cl^- type interactions, which is indeed corroborated by the *S* values obtained at room temperature. The significant differences detected, for the same temperature, from putrescine dihydrochloride to spermine tetrahydrochloride are clear evidence of the effect of both the polyamine chain length and the number of amine/imine groups on the conformational behaviour of these molecules. In fact, this is in close accord with the x-ray data reported in the literature,[42] which indicate an extended all-*trans* geometry for the polyamines under study, and only a slightly twisted orientation (one *gauche* tilt) for the hydrochloride form of the tetraamine spermine.

The agreement between the Raman experimental and calculated values was found to be fairly good for the CH_2 vibrational modes, as opposed to the NH(ND)/NH_2(ND_2) vibrations and in particular to the NH_2^+ (ND_2^+) /NH_3^+ (ND_3^+) modes. In fact, the latter are significantly more influenced by intermolecular interactions (owing to the presence of the Cl^- counterion), not considered in the theoretical study presently carried out. Also, the wavenumber values for the CH_2 stretching modes affected by Fermi resonance interactions are not obtained accurately through *ab initio* calculations, which explains the gap detected between the experimental and theoretical results for these oscillators (e.g. the band observed at 2846 cm^{-1} vs that calculated at 2890 cm^{-1}, and the band observed at 2860 cm^{-1} vs that calculated at 2918 cm^{-1}, for *N*-hydrogenated putrescine, Table 1). Moreover, this observed experimental shift for lower wavenumbers is in total accord with the presently proposed Fermi resonance mechanism, responsible for a red shift of the CH_2 symmetric fundamental mode and a blue shift of the corresponding overtones (which are thus overruled by the CH_2 antisymmetric bands).

CONCLUSIONS

The analysis of the Raman spectra, in the high-wavenumber region, of the biologically relevant polyamines putrescine, spermidine and spermine, and of their hydrochloride salts, in both the undeuterated and *N*-deuterated forms, was performed, for the solid and liquid states, and the results were compared with those from previously reported studies on similar systems.

A complete assignment of the N–H, C–H and N–D stretching modes is presented. It was found that nitrogen protonation (giving rise to of N^+—H···Cl^- interactions) is responsible for important changes in both the intensity and wavenumber of the N–H/N–D stretching bands. For the C–H stretching modes, it was verified that deuteration of the amino groups does not affect significantly either the wavenumbers or the number of Raman signals observed. Ionization of the polyamines (through *N*-protonation), in turn, leads to a general shift to higher wavenumbers of the CH_2 stretching vibrations, their intensity remaining virtually unaffected.

The conformational characteristics of the three polyamines under study were investigated, in particular the *trans*/*gauche* ratio, as a function of the length of their hydrocarbon chain (between nitrogens), and of the temperature (physical state of the sample), following the Gaber and Peticolas procedure. It was concluded that nitrogen deuteration seems to be responsible for an increased degree of *gauche* conformation within the chain, as the *N*-hydrogenated species correspond to a tighter arrangement in the solid. In the crystalline hydrochloride salts, in turn, the high *S* values calculated indicate a clear predominance of the all-*trans* geometry. The results obtained for putrescine, spermidine and spermine show that these compounds usually display an all-*trans* conformation in the solid state (except for the *N*-protonated tetraamine spermine), which was found to decrease in the liquid.

Acknowledgements

The authors acknowledge financial support from the Portuguese Foundation for Science and Technology, within the project POCTI/33199/QUI/2000, co-financed by the European Community Fund FEDER.

REFERENCES

1. Bertoluzza A, Fagnano C, Finelli P, Morelli MA, Simoni R, Tosi R. *J. Raman Spectrosc.* 1983; **14**: 386.
2. Chang SC, Kang BG. *J. Plant Physiol.* 1999; **154**: 463.
3. Oh TJ, Kim IG. *Biotechnol. Tech.* 1998; **12**: 755.
4. Batista de Carvalho LAE, Lourenço LE, Marques MPM. *J. Mol. Struct.* 1999; **482–483**: 639.
5. Marques MPM, Batista de Carvalho LAE. In *COST 917: Biogenically Active Amines in Food*, vol. 4, Morgan DML, White A, Sanchez-Jimenéz F, Bardocz S (eds). European Commission: Luxembourg, 2000; 122.
6. Marques MPM, Batista de Carvalho LAE, Tomkinson J. *J. Phys. Chem. A* 2002; **106**: 2473.

7. Amorim da Costa AM, Marques MPM, Batista de Carvalho LAE. *Vib. Spectrosc.* 2002; **29**: 61.
8. Ghazanfar SAS, Edsall JT, Myers DV. *J. Am. Chem. Soc.* 1964; **86**: 559.
9. Frisch MJ, Trucks GW, Schlegel HB, Scuseria GE, Robb MA, Cheeseman JR, Zakrzewski VG, Montgomery Jr. JA, Stratmann RE, Burant JC, Dapprich S, Millam JM, Daniels AD, Kudin KN, Strain MC, Farkas O, Tomasi J, Barone V, Cossi M, Cammi R, Mennucci B, Pomelli C, Adamo C, Clifford S, Ochterski J, Petersson GA, Ayala PY, Cui Q, Morokuma K, Malick DK, Rabuck AD, Raghavachari K, Foresman JB, Cioslowski J, Ortiz JV, Baboul AG, Stefanov BB, Liu G, Liashenko A, Piskorz P, Komaromi I, Gomperts R, Martin RL, Fox DJ, Keith T, Al-Laham MA, Peng CY, Nanayakkara A, Challacombe M, Gill PMW, Johnson B, Chen W, Wong MW, Andres JL, Gonzalez C, Head-Gordon M, Replogle ES and Pople JA. *Gaussian 98, Revision A.3*. Gaussian: Pittsburgh PA, 1998.
10. Russo TV, Martin RL, Hay PJ. *J. Phys. Chem.* 1995; **99**: 17 085.
11. Ignaczak A, Gomes JANF. *Chem. Phys. Lett.* 1996; **257**: 609.
12. Cotton FA, Feng X. *J. Am. Chem. Soc.* 1997; **119**: 7514.
13. Wagener T, Frenking G. *Inorg. Chem.* 1998; **37**: 1805.
14. Ignaczak A, Gomes JANF. *J. Electroanal. Chem.* 1997; **420**: 209.
15. Cotton FA, Feng X. *J. Am. Chem. Soc.* 1998; **120**: 3387.
16. Lee C, Yang W, Parr RG. *Phys. Rev. B* 1988; **37**: 785.
17. Miehlich B, Savin A, Stoll H, Preuss H. *Chem. Phys. Lett.* 1989; **157**: 200.
18. Becke A. *Phys. Rev. A* 1988; **38**: 3098.
19. Becke A. *J. Chem. Phys.* 1993; **98**: 5648.
20. Hariharan PC, Pople JA. *Theor. Chim. Acta* 1973; **28**: 213.
21. Peng C, Ayala PY, Schlegel HB, Frisch MJ. *J. Comput. Chem.* 1996; **17**: 49.
22. Scott AP, Radom LJ. *Phys. Chem.* 1996; **100**: 16502.
23. Dollish FR, Fateley WG, Bentley FF. *Characteristic Raman Frequencies of Organic Compounds*. Wiley: London, 1974.
24. Mureinik RJ, Scheuermann W. *Spectrosc. Lett.* 1970; **3**: 281.
25. Kalyanasundaram K, Thomas JK. *J. Phys. Chem.* 1976; **80**: 1462.
26. Sabatini A, Califano S. *Spectrochim. Acta* 1960; **16**: 677.
27. Diot A, Theophanides T. *Can. J. Spectrosc.* 1972; **17**: 67.
28. Omura Y, Shimanouchi T. *J. Mol. Spectrosc.* 1975; **57**: 480.
29. Giorgini MG, Pelleti MR, Palliani G, Cataliotti RS. *J. Raman Spectrosc.* 1983; **14**: 16.
30. Abbate S, Wunder SL, Zerbi G. *J. Phys. Chem.* 1984; **88**: 593.
31. MacPhail RA, Strauss HL, Snyder RG, Elliger CA. *J. Phys. Chem.* 1984; **88**: 334, and references cited therein.
32. Abbate S, Wunder SL, Zerbi G. *J. Phys. Chem.* 1982; **85**: 3140.
33. Zerbi G, Abbate S. *Chem. Phys. Lett.* 1981; **80**: 455.
34. Mirkin NG, Krimm S. *J. Phys. Chem.* 1993; **97**: 13 887, and references cited therein.
35. Okabayashi H, Kitagawa T. *J. Phys. Chem.* 1978; **82**: 1830.
36. Teixeira-Dias JJC, Batista de Carvalho LAE, Amorim da Costa AM, Lampreia IMS, Barbosa EFG. *Spectrochim. Acta Part A* 1986; **42**: 589.
37. Batista de Carvalho LAE, Amorim da Costa AM, Teixeira-Dias JJC, Barbosa EFG, Lampreia IMS. *J. Raman Spectrosc.* 1987; **18**: 115.
38. Amorim da Costa AM, Batista de Carvalho LAE, Teixeira-Dias JJC, Barbosa EFG, Lampreia IMS. *Can. J. Chem.* 1987; **65**: 384.
39. Minoni G, Zerbi G. *J. Phys. Chem.* 1982; **86**: 4791.
40. Zerbi G, Minoni G, Tulloch MP. *J. Chem. Phys.* 1983; **75**: 5853.
41. Gaber BP, Peticolas WL. *Biochim. Biophys. Acta* 1977; **465**: 260.
42. Giglio E, Liquori AM, Puliti R, Ripamonti A. *Acta Crystallogr.* 1966; **20**: 683.